CTU Journal of Innovation and Sustainable Development
ISSN 2588-1418 | e-ISSN 2815-6412

DOI:10.22144/ctujoisd.2025.014

Optimal location and size of electric vehicle charging and discharging stations in distribution networks with integrated distributed generations

Vo Minh Thien[1,2*], Tran Thi Lan Anh[2], Nguyen Quang Ai[2], Tran Trung Khanh[2], and Vo Ngoc Dieu[1,3]

[1]*Department of Power Systems, Ho Chi Minh City University of Technology (HCMUT), Viet Nam*

[2]*Research Space for New Energy Development, Department of Electrical - Electronic - Telecommunication, Can Tho University of Technology, Viet Nam*

[3]*Viet Nam National University Ho Chi Minh, Viet Nam*

**Corresponding author (vmthien.sdh222@hcmut.edu.vn)*

Article info.

Received 24 Aug 2024
Revised 7 Oct 2024
Accepted 13 Feb 2025

Keywords

Electric vehicle, EVCS, V2G, Optimal location EV

ABSTRACT

Nowadays, the world is moving towards green energy vehicles and electric vehicles (EVs) are one of the chosen solutions. Vehicle-to-grid (V2G) technology is gradually gaining attention to support issues of performance optimization, energy fluctuations, reducing grid operating costs and bringing optimal efficiency to owners. Along with the rapid increase in the number of EVs, the deployment of effective electric vehicle charging station (EVCS) infrastructure is desirable. However, improper installation can cause many negative impacts on the grid and vice versa, especially EVCS applying V2G charging and discharging techniques. In this study, we propose a computational model to determine the optimal location and size of EVCS applying V2G technique in a distribution network integrating distributed generation sources (DG) with the goal of minimizing active power loss, using an improved method combining the firefly algorithm with the quantum-inspired evolutionary algorithm (QBFA) to find solutions for the problem. The solution results are simulated on a 33-node IEEE standard distribution network using Matlab software and compared with the original FA algorithm to evaluate and propose computational solutions to develop the EVCS system infrastructure in practice.

1. INTRODUCTION

Increasing energy demand, loss gradually fossil fuel sources, and greenhouse gas emissions are major threats the world faces (Singh et al.,2012). The oil consumption in the transportation sector is expected to rise by 54% by 2035 (Matsuo et al., 2013). The transportation sector currently accounts for about 23% of global greenhouse gas emissions, and thus significant improvements are needed in the sector to limit global warming to 2°C (Cazzola et al., 2016). The most effective way to reduce greenhouse gas emissions in the transportation sector is to replace internal combustion engine (ICE) vehicles with low-emission or zero-emission electric vehicles (EVs) (Graham-Rowe et al., 2012). Electric vehicles have the potential to control greenhouse gas emissions, which are the causes of climate change and global warming. In addition to environmental aspects, lower operating costs, noise, and maintenance are additional benefits influencing many countries to transition from ICE vehicles to electric vehicles (Teixeira & Sodré, 2016). Currently, renewable energy systems (such as solar, wind, etc.) are being connected to the grid in large numbers. Due to the natural intermittency of renewable energy causing fluctuations in electricity generation, compensating from other energy sources (e.g., battery energy storage systems) is essential to adjust the natural variability of renewable energy, ensure grid frequency stability, and mitigate the impact of reverse voltage increase caused by current flow. The Vehicle-to-Grid (V2G) system is proposed to address these issues as an essential solution when EV charging stations (EVCS) need to be arranged to support this development, and intermittent charging times can pump power back into the grid to ensure the system operates stably, maximize renewable energy utilization, and optimize operation. Its core is to use the energy storage of a large number of electric vehicles as a buffer storage for the grid and renewable energy. The energy storage of EVs will provide power and support for the grid, such as peak shaving, reactive power compensation, etc. When grid load is low, it is used to store electricity to avoid wastage. However, EVs cannot be connected to the grid at will without management. This is because if the grid is at peak load while also bearing the charging demands of a large number of vehicles, it will certainly have a very severe impact on the grid. For EVs, in addition to supporting the grid, they must also meet daily travel needs. Therefore, during grid supply, the energy storage of EVs must also be considered to avoid affecting normal usage. Thus, researching V2G systems to coordinate charging and discharging between EVCS and the grid is essential to not affect the operation of the grid and not restrict the normal usage of both the grid and transportation (Liu et al., 2012).

Well-planned distribution of charging stations will lead to an improved charging system that adequately meets the energy demand for EV loads (Chinnam & Murat, 2016). The location of charging stations plays a crucial role affecting various aspects of the power grid. The optimal location of EVCS can not only reduce power losses and voltage deviations but also improve accessibility (Islam et al., 2015). As EVs are widely adopted, it will increase the burden on public charging stations. Therefore, the location of the charging stations must ensure that vehicles can easily move within the area (Islam et al., 2018). Some studies have focused on minimizing the impact of electric vehicles on the power system. In (Deilami et al., 2011), the authors present a smart, sustainable load balancing control method to reduce power losses and improve system voltage. Reactive power adjustment is used in EVCS to enhance voltage configuration (Yong et al., 2015). The reliability and economic-technical benefits of integrating DG have been demonstrated (Dixit et al., 2017). Therefore, integrating DG has been proposed as a feasible method to mitigate the impacts of EV charging (Shaaban et al., 2012).

The paper (Farsadi et al., 2015)**,** presents a method for optimizing the location and operation of DG in a distribution system considering the cost objective function for power loss. One of the most important tasks in operating a distribution system is to develop a suitable plan. The objective function is a nonlinear problem (NLP) solved using a genetic algorithm (GA). In this way, GA is suitable for carefully analyzing the search space and then finding optimal solutions. The paper (Boonluk et al., 2020) presents a method for optimizing the location and capacity of DG installation in a distribution system, considering the cost objective function of voltage deviation, power loss, and peak load coverage. The simulation results of the installation are evaluated in a 33-bus IEEE distribution network. The Particle Swarm Optimization (PSO) algorithm has been applied to solve this optimization problem. The objective function considered for minimization is the total cost incurred in the distribution network, including voltage deviation cost, power loss, and peak demand. The installation of DG was operated in the IEEE-33 bus distribution network using GA and PSO algorithms to optimize the objective function, and results from both showed that DG installation could improve the efficiency of the distribution network in terms of reducing costs, voltage deviation, power loss, peak demand, and effectively supporting the connection of renewable energy sources with fluctuations in electricity generation.

Determining the location of each EVCS aims to enhance efficiency, such as minimizing voltage deviation, power loss, and peak demand (load peak) in the distribution network. Furthermore, comparing different optimization algorithms has not been studied to verify the simulation results obtained. Therefore, our proposed problem is to find the optimal location of EVCS in a distribution network integrated with renewable energy connected to areas with fluctuating load demand over a 24-hour period using the improved QBFA algorithm derived from the original FA algorithm, with the objective function of minimizing costs including; voltage deviation cost, power loss, and peak demand. The proposed solution is evaluated and tested through simulations using Matlab software on a standard IEEE 33-bus distribution network integrated with distributed power sources, and the problem solution is assessed, analyzed, and proposed as the best solution for design and economic operation in EVCS infrastructure development.

The Firefly Algorithm (FA) is an optimization algorithm inspired by the communication behavior of fireflies. This algorithm is classified as a metaheuristic and is applied to tackle optimization problems in complex search spaces, especially in engineering and computational fields. (Cheung et al., 2014)

The Firefly Algorithm with Quantum Bit (QBFA) is a variant that combines the traditional Firefly Algorithm with the fundamental principles of quantum computing. Integrating quantum mechanics into the Firefly Algorithm enhances its ability to explore the search space more quickly and efficiently, particularly in complex optimization problems. (Zitouni et al., 2021)

Contributions of the paper:

– Efficiently building an optimization problem for minimizing voltage deviation and power loss, with constraints on power, charging/discharging energy, and efficiency in the considered cycle.

– First-time application of FA algorithm to determine the optimal location of each charging station in the distribution system.

– Utilization of MATPOWER/MATLAB R2022A to simulate and solve the optimization problem of location using FA and QBFA algorithms in the IEEE 33-bus distribution network.

The structure is divided into 6 sections: section 1 introduction provides an overview of the research and the context of the study; section 2 problem description, defines and outlines the problem being addressed, section 3 discusses the Firefly Algorithm; section 4. algorithm diagram illustrates the proposed algorithm with a diagrammatic representation; section 5 simulation results present the results obtained from simulations; section 6 discussion evaluations based on the simulation results and the effectiveness of the proposed solutions.

2. PROBLEM DESCRIPTION

2.1. Objective function

The main objective of this work is to minimize certain costs incurred in the distribution network (C_{system}), including voltage regulation cost (C_{VR}), energy loss cost (C_{Loss}), and peak load demand cost (C_P) under the condition of delayed infrastructure development. Equation represents the objective function, and some of these costs can be found using equation:

$$\left(C_{IF}\right) = min\left(C_{\text{system}}\right) \tag{2.1}$$

$$C_{\text{system}} = C_{VR} + C_{\text{Loss}} + C_P \tag{2.2}$$

$$C_{VR} = \sum_{t=1}^{T}\sum_{i=1}^{N}\left|V_i - V_{ref}\right| * \gamma_{VR} \tag{2.3}$$

$$C_{Loss} = \sum_{t=1}^{T}\sum_{i=1}^{N}\left|L_{Lineloss}\right| * \gamma_{Loss} \tag{2.4}$$

$$C_P = P_{max} \times \Delta\text{t} \times \gamma_P \tag{2.5}$$

In which $N, V_i, V_{ref}, M, L_{LineLoss}$, P_{max}, γ_{VR}, γ_{Loss} and γ_P are the total number of buses, voltage magnitude (per unit) at bus i, reference voltage equal to 1 pu, total number of branches, active power loss in each branch, maximum active power at the slack bus during the considered time period, voltage regulation cost ratio, energy loss cost ratio, and peak demand cost ratio γ_{VR} = 0.142 \$/p.u (Coello, 2002), γ_{loss} = 0.284 \$/ kWh (Michalewicz & Janikow, 1991), γ_P = 200 \$/kWh/year (Michalewicz & Janikow, 1991), respectively.

2.2. Constraints of the objective function

(1) Voltage constraints: The voltage at each bus must be limited within the lower and upper bounds throughout the considered time period, set at ±5% of the nominal voltage as represented by the equation.

$$V_{lower} \le V_i^t \le V_{upper} \tag{2.6}$$

Where V_{lower} và V_{upper} are the lower and upper voltage limits at bus i, respectively, and V_i^t is the voltage magnitude at bus i at time t.

(2) Battery storage constraints: The power and capacity of the battery are limited to ensure that the operation of the station does not exceed boundary limits during charging or discharging, which can be represented by the equation below.

$$P_{B-min} \le P_{cha}^t, P_{dis}^t \le P_{B-max} \tag{2.7}$$

$$E_{B-min} \le E_b^t \le E_{B-max} \tag{2.8}$$

Where P_{B-min}, P_{B-max} are the minimum and maximum power of the battery, respectively. P_{cha}^t, P_{dis}^t are the charging and discharging rates of the station at time t, respectively. E_{B-min}, E_{B-max} are the charging and discharging rates of the station at time t, respectively.

3. FIREFLY ALGORITHM

The Firefly Algorithm, proposed by Yang (Yang & He, 2013), is a swarm intelligence-based algorithm. This algorithm draws inspiration from the interaction of fireflies in nature through their light emission. The Firefly Algorithm has been shown to be very effective for global optimization problems (Fister et al., 2013). However, research on using this algorithm for constrained optimization is still quite limited. In nature, fireflies emit light with an intensity proportional to their attractiveness. The intensity of this light changes with distance: fireflies that are closer perceive stronger light and are attracted to each other. This mechanism is simulated in the Firefly Algorithm to search for optimal solutions. This algorithm belongs to the class of metaheuristic algorithms, which are used to solve optimization problems in complex search spaces.

Principles of the Firefly Algorithm (Cheung et al., 2014):

Light and Brightness: The brightness of a firefly is proportional to the value of the objective function (the function to be optimized) at its position. Brighter fireflies will attract others towards them.

Attractiveness: The attractiveness between two fireflies is inversely proportional to the distance between them. Fireflies move towards brighter and closer individuals.

Position Update: Each firefly updates its position by moving towards brighter fireflies. This movement follows a calculation formula influenced by the level of attractiveness and a random factor to prevent getting stuck in local optimal.

Additionally, to handle constraints when using swarm algorithms, penalty functions are a common method. This approach is simple, easy to use, and can be applied to all types of constraints (equality or inequality, linear or nonlinear, continuous or discrete). The idea behind this method is to modify the original form of the objective function by adding certain values (called penalty values) to the objective function of individuals that do not satisfy the constraint conditions. If individuals are farther from the feasible region, the penalty values increase, and vice versa. If individuals are within the feasible region, the penalty values are zero. However, the challenge of this method is to determine the penalty coefficient appropriately (Deb, 2000). To address this challenge, in addition to static penalty methods (Fister et al., 2013), many studies have proposed complex methods to determine the penalty coefficient used in penalty functions, such as dynamic penalty methods (Joines & Houck, 1994), self-adaptive penalty functions (Bean & Hadj-Alouane, 1992). Michalewicz (Michalewicz & Janikow, 1991) suggests using a penalty coefficient (static penalty function) because dynamic penalty methods often yield different results for different problems. Coello (Coello, 2002) compares methods using penalty functions with evolutionary algorithms and indicates that determining the penalty coefficient for penalty functions must depend on the specific problem. However, there is very little experimental research evaluating the effectiveness of different types of penalty functions for optimization problems.

3.1. The basic expressions of the Firefly Algorithm

Voltage Constraints: Maintain the voltage at each bus in the power system within the prescribed limits to ensure that the voltage does not exceed the upper bound or fall below the lower bound. This is crucial for protecting equipment and maintaining the stability of the power system. The ±5% limit relative to the nominal voltage is a common standard in electrical systems. Oltage constraints help ensure system stability and safety throughout the operational period.

$$V_{lower} \le V_i^t \le V_{upper} \tag{3.1}$$

Battery Storage Constraints: Ensure that the battery's power and capacity limits are maintained so that the operation of the charging station does not exceed boundary limits during charging or discharging. This is essential for extending the battery's lifespan and preventing unwanted energy losses. Battery storage constraints optimize battery performance, ensuring that charging and discharging processes remain within the permissible power and capacity limits.

$$P_{B-min} \le P_{cha}^t, P_{dis}^t \le P_{B-max} \tag{3.2}$$

$$E_{B-min} \le E_b^t \le E_{B-max} \tag{3.3}$$

Modeling constrained optimization problems

Minimization:

$$f(x_1, x_{2,} \dots x_d), d = 1,2, \dots, D \tag{3.4}$$

Subject to constraints:

$$g_q(x_1, x_{2,} \dots x_d) \leq 0 \quad (3.5)$$

$$h_r(x_1, x_{2,} \dots x_d) = 0 \quad (3.6)$$

$$x_d^L \leq x_d \leq x_d^U \quad (3.7)$$

with q=1,2,..., M; r = 1,2,...., N.

Where: $f(x_1, x_{2,} \dots x_d)$ is the objective function, usually representing losses or voltage fluctuations, $(x_1, x_{2,} \dots x_d)$ are the design variables, $g_q(x_1, x_{2,} \dots x_d)$ and $h_r(x_1, x_{2,} \dots x_d)$are the constraints (regarding stress, deformation), x_d^L and x_d^U are the lower and upper bounds of the design variable x_d, D is the number of design variables; M and N are the numbers of inequality and equality constraints, respectively.

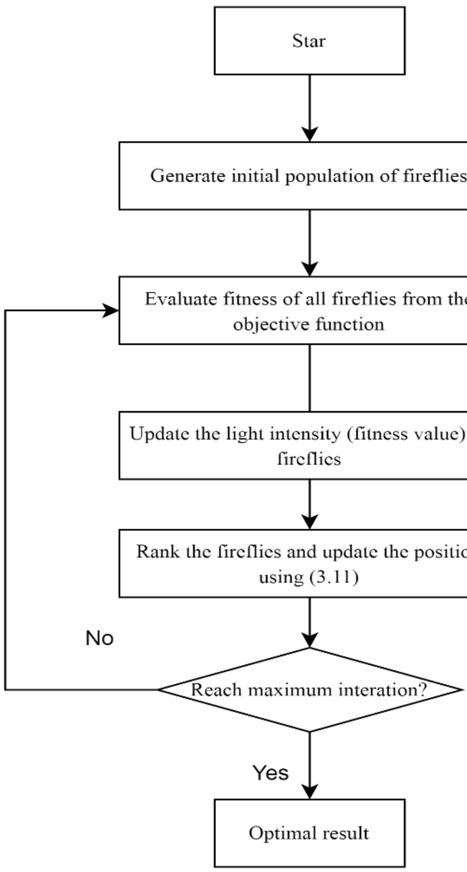

Figure 1. Flowchart of the Firefly Algorithm

*** Firefly Algorithm**

Start the algorithm

Define the objective function *(x)*, in which $x = (x_1, x_2, \dots, x_d)$

Initialize the population of fireflies

Calculate the brightness of each individual *I*

Define the light absorption coefficient *γ*

While (*t* < maximum number of iterations)

For *i* = *1* to *n* (*n* = number of individuals)

For *j* = *1* to *n* (*n* = number of individuals)

If $(I_j > I_i)$ move individual *i* closer to individual *j*

End *if*

Evaluate the new individuals and update brightness

End for *j*

End for *i*

Rank the fireflies and find the best individual

End while

End of the algorithm

The brightness *I* is calculated as follows:

$$I = I_S e^{-\gamma r 2} \quad (3.8)$$

In which, I_S = is the brightness at the light source; γ = is the light absorption coefficient; r = is the distance to the light source.

Since the attraction of a firefly is proportional to the light it emits, the attraction of a firefly (denoted as β) is defined as:

$$\beta = \beta_0 e^{-\gamma r 2} \quad (3.9)$$

The distance between firefly *i* at position x_i and firefly *j* at position x_j is calculated as follows:

$$r_{ij} = \|x_i - x_j\| = \sqrt{\textstyle\sum_{k=1}^{d} (x_{ik} - x_{jk})^2} \quad (3.10)$$

In which, d = is the dimensionality of the search space; ||.|| is denotes the Euclid distance.

The movement of firefly *i* attracted by a brighter firefly *j* is defined as follows:

$$x_i = x_i + \beta_0 e^{-\gamma r_{ij} 2} (x_i - x_j) + \alpha(rand - 0.5) \quad (3.11)$$

In which, x_i^{g+1} and x_i^g are the positions of firefly *i* at iteration *g+1* and g, respectively; x_i^g is the position of firefly *j* at iteration *g+1* and *g; γ* is the light absorption coefficient (0.1 ~ 10); β_0 is the attractiveness at $r_{ij} = 0$; α is the coefficient affecting the random movement of fireflies; *rand* = 1 is a random number from a uniform distribution.

Constrained optimization is a common problem in optimization. To handle constraints when using the Firefly Algorithm, it is necessary to use penalty functions. The reason is that this technique is relatively simple and can be applied to all types of constraints. To guide the fireflies into the feasible region, the original form of the objective function is modified by adding penalty values if the individual does not satisfy the constraint conditions. When the individuals are within the feasible region, the penalty values are zero. For individuals further from the feasible region, the penalty values increase.

To use this method, it is necessary to determine the penalty function value through the penalty coefficient appropriately. Determining the penalty function value depends on the specific optimization problem (Bean & Hadj-Alouane, 1992). To address this issue, different types of penalty functions have been proposed: static penalty functions (Fister et al., 2013), dynamic penalty functions (Join & Houck, 1994), and self-adaptive penalty functions (Bean & Hadj-Alouane, 1992).

Advantages of FA:

1.The algorithm has excellent exploration capabilities in the search space due to the movement of firefly individuals towards brighter ones.

2. It has the ability to avoid local optima thanks to the randomness factor during movement.

3.2. Optimization model based on the Firefly Algorithm and penalty functions

The optimization model based on the Firefly Algorithm and Penalty Functions (FAPF) is illustrated in Figure 2. This model uses the Firefly Algorithm to search for the best choices of design variables within the search space. Additionally, penalty functions are used to handle the constraints of the optimization problem:

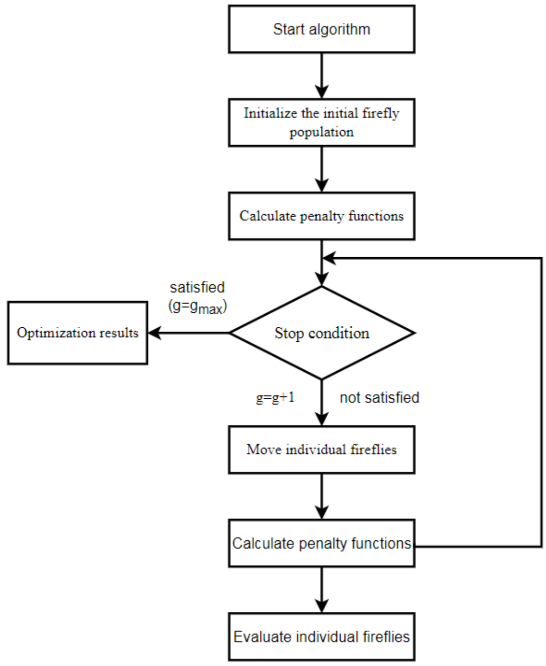

Figure 2. Optimization based on the Firefly Algorithm and penalty functions

Step 1: Start the Algorithm: The algorithm parameters include the maximum number of iterations (g_{max}), the number of fireflies in the population (N), the light absorption coefficient (γ), the type and parameters of the penalty function specified at this step. Typically, these parameters can be set as follows: N = 5*d*, In whith *d* is the number of design variables. γ = 1. g_{max} needs to be sufficiently large to ensure that the optimization process converges.

Step 2: Initialize the Initial Firefly Population: The firefly individuals in the first iteration are initialized randomly within the allowable range of each design variable. At this step, the firefly population is also evaluated using the objective function combined with the values of the penalty functions.

Step 3: Check Stopping Criteria: If the current iteration $g < g_{max}$ the optimization process continues. When the stopping criteria are met, the best design variable has been found by the algorithm.

Step 4: Move the Firefly Individuals: The fireflies move towards other brighter fireflies. If no brighter firefly is found, the individual will move randomly within the search space.

Step 5: Evaluate the Firefly Individuals: The individuals will be evaluated and ranked to identify better individuals. The information of the best individual will be recorded.

3.3. Firefly Algorithm with Quantum Bit

Quantum-Inspried evolutionary algorithm – QEA

Start the Algorithm

Begin $t \leftarrow 0$

1. Initialize *Q(t)*
2. Compute *P(t)* based on the state of *Q(t)*
3. Evaluate *P(t)*
4. Store the best value of *P(t)* in *B(t)*

While (stopping condition is not satisfied)

Begin $t \leftarrow t + 1$

5. Compute *P(t)* based on the state of *Q(t − 1)*
6. Evaluate *P(t)*
7. Update *Q(t)* using Q-gates
8. Store the best value between *B(t − 1)* and *P(t)* in *B(t)*
9. Store the best value of *b* in *B(t)*
10. **If** (stopping condition is satisfied)

Then (move *b* or b_j^t in *B(t)* globally or locally)

End

End

End of the Algorithm

QEA is a probabilistic algorithm similar to other evolutionary algorithms. However, QEA maintains a population of Q-bit individuals Q(t) = $\{q_1^t, q_2^t, \ldots, q_n^t\}$ at generation *t*, whith *n* is the population size and q_j^t is a Q-bit individual defined as:

$$q_j^t = \begin{bmatrix} \alpha_{j1}^t & \alpha_{j2}^t & \cdots & \alpha_{jm}^t \\ \beta_{j1}^t & \beta_{j2}^t & \cdots & \beta_{jm}^t \end{bmatrix} \quad (3.12)$$

In which *m* is the number of Q-bits, the length of the string for each Q-bit and $j = 1,2, \ldots, n$.

Step 1. α_i^0 and β_i^0 which $i = 1,2, \ldots, m$ of all $q_j^0 = q_j^t\big|_{t=0}$ which $j = 1,2, \ldots, n$ are initialized to a value of $1/\sqrt{2}$. This means that a Q-bit individual, q_j^0 represents a linear superposition of all possible states with a uniform probability.

$$\left|\psi_{q_j^0}\right\rangle = \sum_{k=1}^{2^m_{k=1}} \frac{1}{\sqrt{2^m}} |X_k\rangle \quad (3.13)$$

In which X_k is the k state represented by a binary string $(x_1 x_2 \ldots x_n)$ where x_i for $i = 1,2, \ldots, m$ is either 0 or 1 according to the probabilities $\left|\alpha_i^0\right|^2$ and $\left|\beta_i^0\right|^2$

Step 2: This step calculates the binary values in $P(t)$ by observing the states of $Q(0)$, where $P(0) = \{x_1^0, x_2^0, \ldots, x_n^0\}$ at $t = 0$. A binary solution, x_j^0 for $j = 1,2, \ldots, n$ is a binary string of length m, formed by selecting 0 or 1 for each bit using the probabilities, $|\alpha^0|^2$ or $|\beta^0|^2$ whith i = 1,2, … , m of q_j^0.

Step 3: Each binary solution x_j^0 is evaluated to determine its fitness.

Step 4: The initial best solutions are then selected from the binary solutions in P(0) and stored in *B(0)* where *B(0)=*$\{b_1^0, b_2^0 \ldots, b_n^0\}$ *and* $b_j^0 = b_t^0|_{t=0}$ is the same as the initial generation x_j^0.

Steps 5 + 6: In the while loop, the binary solutions in *P(t)* are formed by observing the states *Q(t - 1)* as in Step 2, and each binary solution is evaluated for its fitness. It is important to note that x_j^t in *P(t)* may be formed by multiple observations of q_j^{t-1} in *Q (t - 1)*. In this case, x_j^t should be replaced by x_{jl}^t, where l is an observation index.

Step 7: In this step, the Q-bit individuals in *Q(t)* are updated by applying the Q-gates defined in formula (3.12).

Steps 8 + 9: The best solutions among *B(t − 1)* and *P(t)* are selected and stored into *B(t)*. If the best solution stored in *B(t)* is better than the best solution stored in *b*, the solution stored in *b* will be replaced with the new value.

Step 10: If a move condition is satisfied, then the best solution bbb will be moved to *B(t),* or the best solution among several solutions in *B(t)* will be moved to them. The move condition is a design parameter, and the moving process described below may result in a change in the probability of a Q-bit individual.

The binary solutions in *P(t)* are discarded at the end of the loop because *P(t+1)* will be generated by observing the updates in Step 7. Until the termination condition is met, QEA runs in the while loop.

The Firefly Algorithm with Quantum Bit (QBFA) (Zitouni et al., 2021). It is a hybrid variation of the traditional firefly algorithm and the fundamental principles of quantum computing. The integration of quantum mechanics into the firefly algorithm enhances its ability to explore the search space more quickly and efficiently, especially in complex optimization problems., but it incorporates quantum concepts to adjust how fireflies update their positions and interact with one another:

1. Quantum state initialization: Each firefly is represented as a qubit, with its state described by a quantum wave function. These qubits represent the firefly’s position in the search space, and the firefly’s state is a superposition of multiple possible locations.

2. Updating brightness based on wave function: The brightness of a firefly is determined not only by the value of the objective function but also by the quantum superposition of its state. When brighter fireflies are found, weaker ones adjust their wave functions to move toward them.

3.Utilizing quantum interference: Instead of simply moving based on distance like in the traditional algorithm, QBFA leverages principles such as quantum interference and measurement to create nonlinear movements. This allows fireflies to “jump” to more promising regions in the search space.

4. Heisenberg uncertainty and quantum qandomness: Movement is no longer fixed, as it is in the traditional algorithm. Due to the Heisenberg uncertainty principle, there is a degree of randomness in the position and momentum of fireflies, allowing them to escape local optima and explore the search space more comprehensively.

5. Measurement: After fireflies move through the search space, the measurement process is applied to determine the actual position of each firefly. This means transitioning from a superposition state to a specific position in the search space. The measurement collapses the quantum state, revealing the firefly’s exact location, which is then used in the optimization process. This step ensures that a potential solution is selected from the quantum possibilities.

Advantages of QBFA

Better global search capability: Thanks to quantum superposition and randomness, the Firefly Algorithm with Quantum Bit (QBFA) can explore the global search space more efficiently compared to the traditional Firefly Algorithm (FA).

Minimizing local optima trapping: Due to quantum uncertainty and randomness, fireflies have the ability to escape local optima, thereby increasing the chances of finding the global optimal solution.

Faster optimization: Quantum interference and state superposition accelerate convergence, particularly in complex search spaces with numerous local optimal.

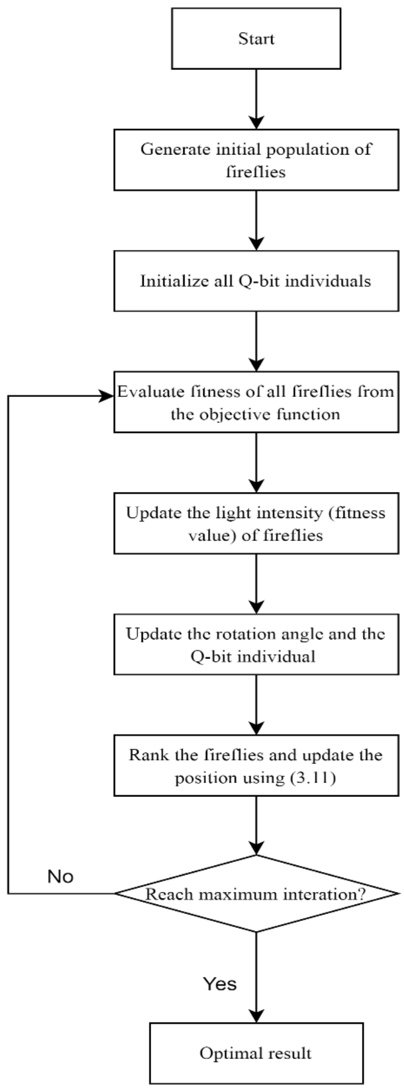

Figure 3. Diagram of the QBFA Algorithm

4. THE PROCESS OF MODEL EXPRESSED IN THE STEPS

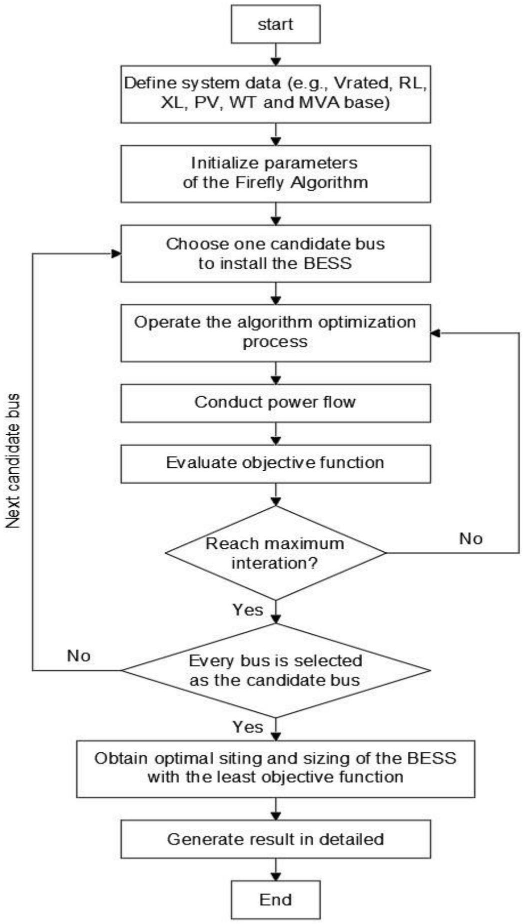

Figure 4. Algorithm Diagram

*Step 1***:** Identify the input data for the problem, includingV_{rated}, RL, XL, PV, WT and MV_{base} to simulate the IEEE distribution network in Matpower.

*Step 2***:** Initialize the parameters for the Firefly Algorithm.

*Step 3***:** Select a bus location to install the charging station (from bus 2 to bus 33).

*Step 4***:** Run the algorithm to solve the optimization problem.

*Step 5***:** Optimize the power at the selected location.

*Step 6***:** Evaluate the objective function and update with better values.

*Step 7***:** If the maximum number of iterations is reached, proceed to step 8; otherwise, return to step 4.

*Step 8***:** Compare the results at each charging station location chosen in step 3.

*Step 9***:** If the selected bus location is the final position, proceed to step 10; otherwise, return to step 3.

*Step 10***:** Find the optimal location for the charging station where the objective function has the smallest value.

*Step 11***:** Provide the optimal charging station value using the Fourier coefficient method.

5. SIMULATION RESULTS

Input data for the problem includes**:** possible bus locations for station installation (from 2 to 33), maximum charging and discharging power of a station, sampling period, charging and discharging efficiency of the station.

The input data for the IEEE power grid includes branch parameters, load parameters, voltage parameters, maximum and minimum voltages; as well as data on typical load factors and the typical power output of solar and wind sources over 24 hours.

There are two types of distributed energy sources: wind turbines (WT) and photovoltaic (PV) panels connected to the distribution power system. For this problem, the system includes (Boonluk et al., 2020):

– 2 wind turbines located at buses 18 and 24, with a capacity of 1 MW per turbine;

– 3 photovoltaic systems located at buses 5, 21, and 31, with a capacity of 400 kVA per system;

– 4 photovoltaic systems located at buses 8, 12, 28, and 33, with a capacity of 500 kVA per system.

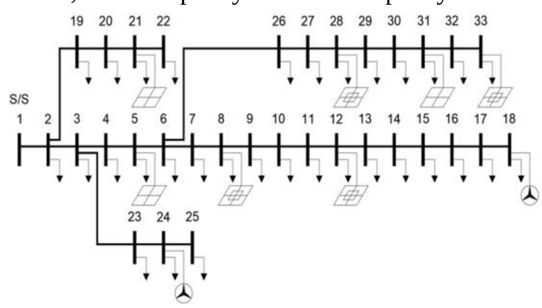

Figure 5. IEEE 33-bus electrical network with distributed energy sources

The typical power output of wind and solar PV sources is referenced according to the following parameter set (Hung & Mithulananthan, 2012):

Table 1. Typical power output of wind and solar photovoltaic sources

Hour	PVs	WTs	Hour	PVs	WTs
12--1 am	0	0.25	12--1	1	0.71
1--2	0	0.235	1--2	0.95	0.805
2--3	0	0.23	2--3	0.83	0.91
3--4	0	0.235	3--4	0.72	0.96
4--5	0	0.22	4--5	0.55	0.86
5--6	0.05	0.225	5--6	0.3	0.81
6--7	0.1	0.19	6--7	0.13	0.7
7--8	0.27	0.17	7--8	0.05	0.585
8--9	0.5	0.25	8--9	0	0.415
9--10	0.7	0.37	9--10	0	0.325
10--11	0.9	0.47	10--11	0	0.29
11--12 pm	0.95	0.62	11--12 am	0	0.265

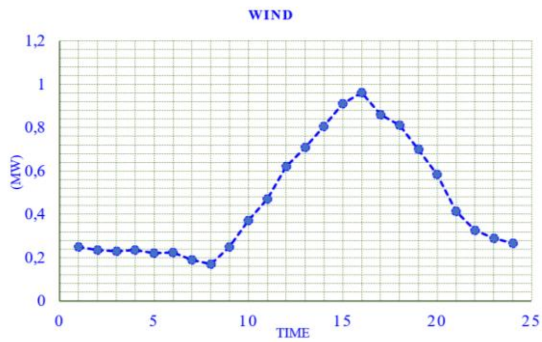

Figure 6. Typical power generation profile of wind power over 24 hours

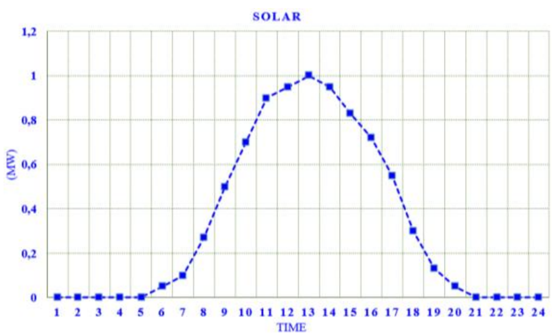

Figure 7. Typical power generation profile of solar power over 24 hours

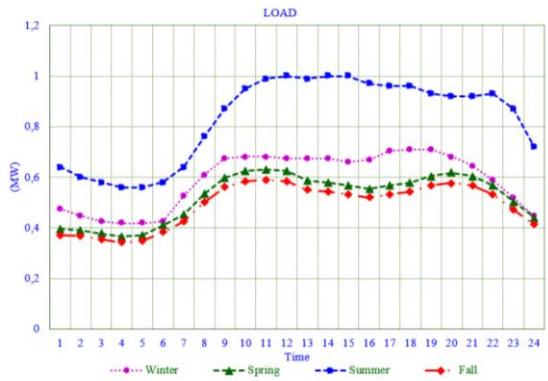

Figure 8. Typical load factor profile for 4 seasons over 24 hours

For radial power networks, the load power values at each node can be calculated based on the voltage magnitude values (Boonluk et al., 2020):

$$P_{L-i} = P_{0i}(a_p + b_p|V_i| + c_p|V_i|^2) \quad (5.1)$$

$$Q_{L-i} = Q_{0i}(a_q + b_q|V_i| + c_q|V_i|2) \quad (5.2)$$

In which, P_{L-i}, and Q_{L-i} represent the real and reactive power at bus *i*, respectively. P_{0i} , Q_{0i} are the initial real and reactive power at bus *i*. The parameters $a_p + b_p + c_p = 1$, $a_q + b_q + c_q = 1$ are coefficients used in the load profile calculation. The base voltage (V_{base}) = 12,66 kV, the base power (MVA_{base}) = 10 MVA. For this power grid, the parameters are set as $ap = aq = 0.4$, $b_p = b_q = 0.3$, and $c_p = c_q = 0.3$. Evaluate the charging station placement at each bus from 2 to 33, compute the cost function for each potential placement, Identify the bus with the lowest optimal cost function as the best location for the charging station.

According to (Baran & Wu, 1989) the typical load profiles are provided for four seasons: spring, summer, autumn, and winter. For this paper, we will use the summer load profile, as it represents the highest and most extreme load scenario for calculations.

Table 2. Typical load factors for four seasons over 24 hours

Time	Winter	Spring	Summer	Autumn	Time	Winter	Spring	Summer	Autumn
12--1 am	0.4757	0.3969	0.6400	0.3717	12--1	0.6745	0.5859	0.9900	0.5487
1--2	0.4473	0.3906	0.6000	0.3685	1--2	0.6745	0.5796	1.0000	0.5428
2--3	0.4260	0.3780	0.5800	0.3540	2--3	0.6603	0.5670	1.0000	0.5310
3--4	0.4189	0.3654	0.5600	0.3422	3--4	0.6674	0.5544	0.9700	0.5192
4--5	0.4189	0.3717	0.5600	0.3481	4--5	0.7029	0.5670	0.9600	0.5310
5--6	0.4260	0.4095	0.5800	0.3835	5--6	0.7100	0.5796	0.9600	0.5428
6--7	0.5254	0.4536	0.6400	0.4248	6--7	0.7100	0.6048	0.9300	0.5664
7--8	0.6106	0.5355	0.7600	0.5015	7--8	0.6816	0.6174	0.9200	0.5782
8--9	0.6745	0.5985	0.8700	0.5605	8--9	0.6461	0.6048	0.9200	0.5664
9--10	0.6816	0.6237	0.9500	0.5841	9--10	0.5893	0.5670	0.9300	0.5310
10--11	0.6816	0.6300	0.9900	0.5900	10--11	0.5183	0.5040	0.8700	0.4720
11--12 pm	0.6745	0.6237	1.0000	0.5841	11--12 am	0.4473	0.4410	0.7200	0.4130

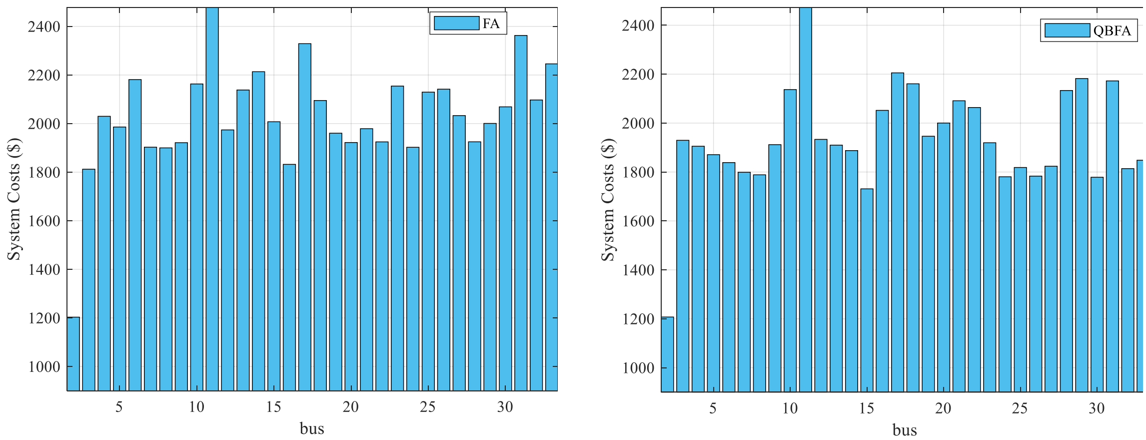

(a) (b)

Figure 9. Cost optimization function results from bus 2 to bus 33 of a) FA, b) QBFA

From the simulation results, the optimal cost function for both algorithms is best at bus 2 (Cost = 1200$).

The results in Figure 9 show that the optimal function achieves the minimum value at the first bus, then increases and stabilizes at $1800 to $2400 at subsequent buses. The analysis focuses on cost fluctuations at the buses and spatial stability.

For the FA, costs vary significantly between buses, ranging from a low of around $1200 to a peak near $2400, with no clear stabilization trend. The FA exhibits stronger cost fluctuations compared to the QBFA, indicating that QBFA may converge faster or better in terms of cost stability after the initial buses.

In contrast, for the QBFA, the graph shows a similar fluctuation, but with a more stable trend, where costs remain within the range of $1800 to $2000 after bus 2, with fewer large variations compared to the FA. QBFA tends to maintain a more consistent cost level after a certain number of buses (after bus 10), whereas FA continues to show noticeable variations between buses.

After bus 2, the system costs fluctuate and increase at other buses. If the objective is to minimize system costs, then bus 2 should be prioritized for EVCS installation. Stability in system cost is an important factor in determining the size and location of the EVCS, then the QBFA algorithm may offer better results than FA.

QBFA has the capability to ensure consistency in reducing power losses at various locations, which is crucial for the planning and operation of distribution systems integrated with EVCS.

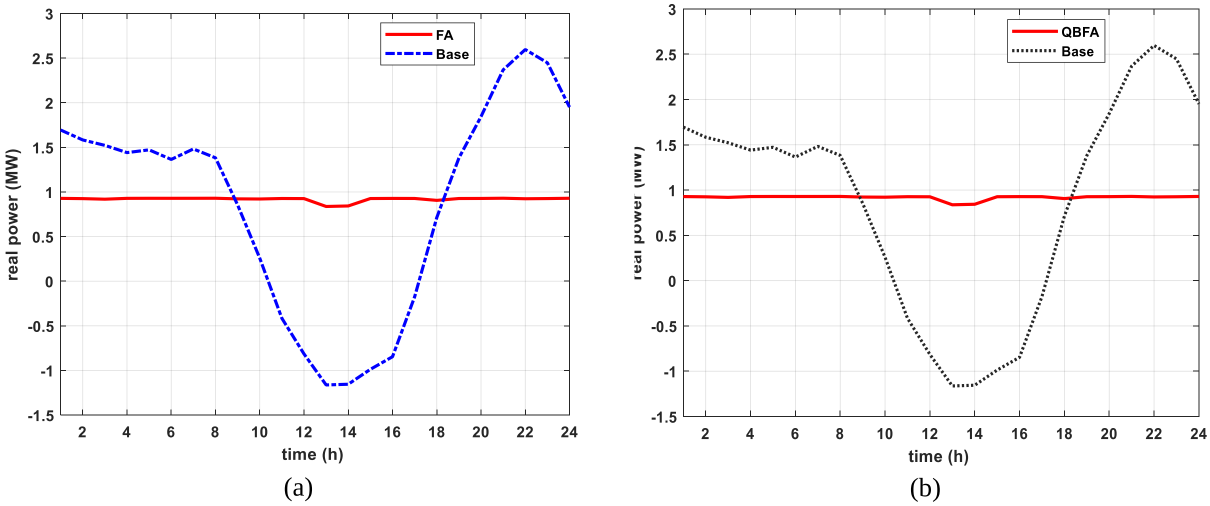

Figure 10. Power P when installing the charging station at bus 2 of a) FA, b) QBFA

Both algorithms reach their peak values around 20:00 to 22:00. FA in chart (a) reaches a higher peak of approximately 2.5 MW, while QBFA in chart (b) has a slightly lower peak, around 2.25 MW. Both algorithms experience a power drop between 10:00 and 12:00. The minimum power in both cases reaches approximately 1 MW. While both algorithms follow a similar overall power pattern, FA exhibits larger fluctuations compared to QBFA. Specifically, FA shows stronger oscillations from 6:00 to 12:00 and reaches a higher peak in the evening. QBFA presents a smoother curve with less fluctuation throughout the day, showing a less significant drop and more stability during peak hours.

Power at the balancing node is also an important issue to consider. Data obtained in Figure 10 indicates that the power changes minimally over 24 hours, providing a stable 1 MW for the load. The results demonstrate the advantage of EVCS in maintaining and balancing power for the system, which is essential for ensuring stability during peak loads and when the grid has excess power.

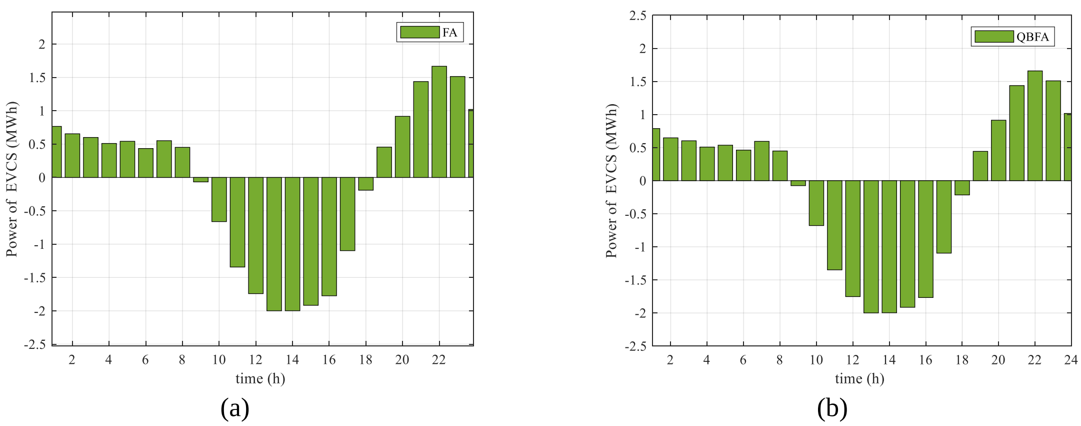

Figure 11. Charging/discharging power of the station over 24 hours at bus 2 of a) FA, b) QBFA

The charging station power is presented in Figure 11, showing the charging or discharging rate for each hour. The maximum discharging power of the station is approximately 1.6 MW at 10 PM when the load is high and wind and solar power generation is low. The maximum charging power is about 2 MWh at 1 PM - 2 PM when wind and solar power sources are near peak. There is no significant difference between the two algorithms when compared about charging/ discharging power of the station over 24 hours at bus 2.

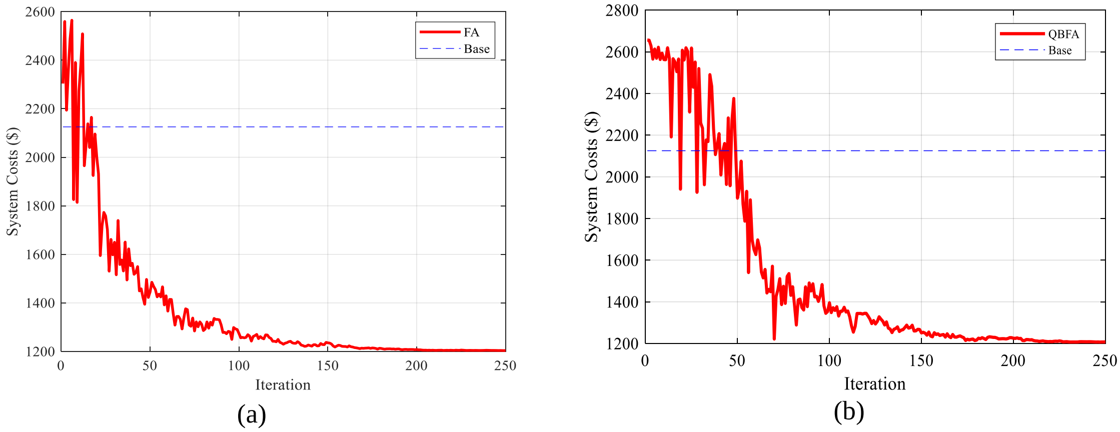

Figure 12. Cost optimization function results at bus 2 through iterations of a) FA, b) QBFA

Figure 12 the analysis focuses on the convergence speed through the number of iterations, reflecting the performance over time. The objective function fluctuates significantly during the first 100 iterations (from \$2600 down to \$1150) in both algorithms. Changing the gamma coefficient from 0.04 to 0.02 to 0.01 (at iteration intervals of 0 - 100 - 200 - 300) helps the system stabilize and approach a better minimum value. Both algorithms start with a high system cost of around \$2600. FA has relatively smoother cost reductions compared to QBFA, especially during the first 50-100 iterations. FA seems to converge faster, reaching stability at around 100 iterations. QBFA shows larger variations in cost in the early stages, which might suggest instability or sensitivity in the optimization process. QBFA converges more slowly, with fluctuations continuing until around 150 iterations, after which it stabilizes. The two algorithms both relatively converge from the 200th iteration onward. QBFA is more computationally complex due to its reliance on quantum mechanics principles. FA may perform better due to its simplicity and efficiency. In some cases, QBFA may struggle with premature convergence to local optima, similar to FA. This can happen if the balance between exploration and exploitation is not well-maintained or if quantum-inspired operators do not sufficiently diversify the search. Research showed that QBFA was more stable than FA in reducing cost fluctuations at different positions (bus). FA has the advantage of fast convergence, making it suitable for problems requiring quick optimization. This is of great significance in problems that require spatial stability. QBFA can ensure that the algorithm explores the search space more comprehensively, especially in complex nonlinear problems. Although QBFA converges slower than FA in the early stages, it has the potential to achieve higher-quality solutions when handling large and complex problems. The use of QBFA in this study was not only aimed at immediate efficiency but also focused on testing and developing a new algorithm with superior potential for more complex problems.

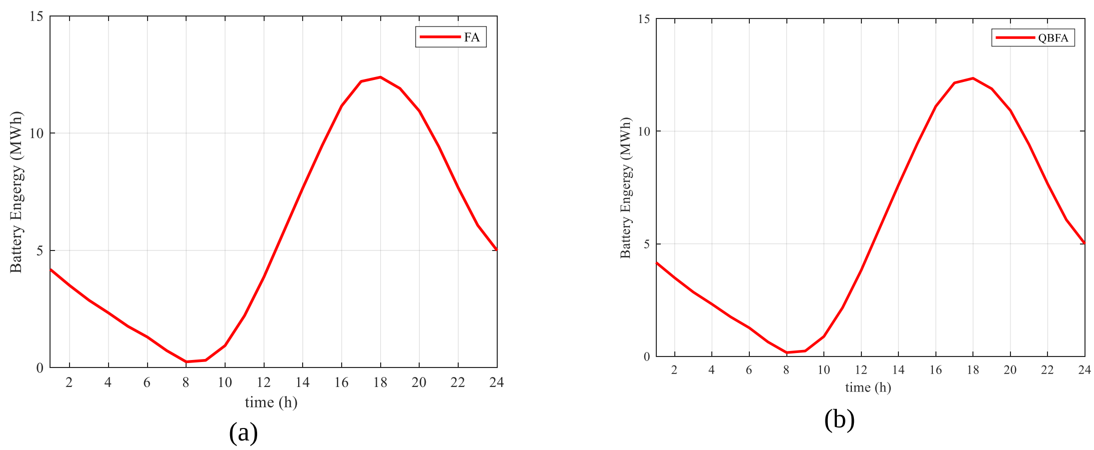

Figure 13. Charging/discharging energy over 24 hours at bus 2 of a) FA, b) QBFA

Data in Figure 13 describes the state of energy (SOE) of the charging station in both algorithms over 24 hours, showing similar patterns. From 1 AM to 8 AM, energy gradually decreases as the station is in a low discharging state. The station transitions from discharging to charging energy between 8 AM and 9 AM and switches back again between 5 PM and 6 PM. The station's energy is lowest at around 0.2 MWh between 8 AM and 9 AM and highest at about 12.25 MWh between 5 PM and 6 PM. -There is no significant difference between the two algorithms when compared at bus 2 about charging/discharging energy over 24 hours.

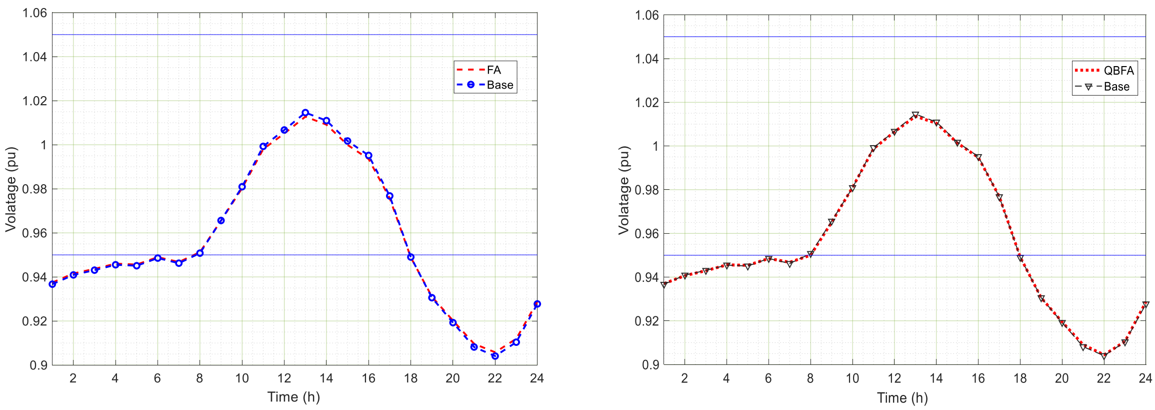

(a) (b)

Figure 14. Voltage in 24 hours at bus 21 of a) FA, b) QBFA

Both algorithms follow a similar voltage fluctuation pattern over time, with a rise in voltage during the middle of the day (around 12:00-14:00) and a drop in the evening and late night (around 20:00-22:00). The maximum voltage in both algorithms occurs at around the same time, peaking between 12:00 and 14:00. However, FA seems to reach a slightly higher peak voltage compared to QBFA, although the difference is minimal. Both charts show a voltage dip in the evening, with the voltage reaching its lowest point between 20:00 and 22:00. The patterns for both algorithms are nearly identical here, with QBFA possibly showing a slightly lower minimum voltage than FA. There is no major difference between the two algorithms when it comes to voltage behavior at bus 21 over 24 hours.

The above voltage distribution value can be seen that the voltage intensity is proportional to the DG capacity mobilized into the system. In this case, it is clear that the time frame from 8:00 to 18:00 is the time frame where the DG capacity from solar power and wind power is loaded into the grid at its highest level. Outside of this time frame, the mobilized capacity decreases, so the voltage intensity also decreases. This is a feature that investors need to care attention to in order to supplement the mobilized capacity from other suitable sources, maintain continuous operation and stabilize the quality of electricity.

6. CONCLUSION

The QBFA algorithm is an enhanced version of the FA algorithm, theoretically expected to yield better results than FA. However, when applied to location for installing evcs on the IEEE 33-bus power grid, only a portion of the algorithm was implemented, specifically the quantum Q-bit rotation gate, which led to less optimal results compared to the FA algorithm. The objective function set for this problem is to minimize the total costs incurred in the distribution power network, including voltage deviation costs, power loss, and peak demand costs. The installation of EVCS operating in the IEEE 33-bus power grid was optimized using both FA and QBFA algorithms to optimize the objective function, and the results were compared to verify the accuracy of both methods. The findings indicate that the installation of EVCS can improve the efficiency of the distribution network by reducing voltage deviation costs, power loss, and peak demand. Additionally, EVCS can support the integration of renewable energy sources, which tend to have fluctuations, into the system.

Through the simulation results, it can be concluded that the model applying QBFA improved from FA is a powerful algorithm, identifying good solutions with fast convergence and meeting the constraints and objectives. In addition to optimizing the location and size of EVCS, it also optimizes the charging and discharging schedule of each EVCS location in the distribution network at each time point in 24 hours. The results indicate that the installation of charging stations can improve operational efficiency, reduce energy loss, effectively mobilize DG sources and peak load demand. EVCS charging and discharging schedule coordination can also support the integration of other highly volatile renewable energy sources, optimizing the use benefits. This solution can serve as a foundation for the development of EVCS infrastructure applying V2G technology in practice.

REFERENCES

Baran, M. E., & Wu, F. F. (1989). Network reconfiguration in distribution systems for loss reduction and load balancing. *IEEE Transactions on Power delivery*, *4*(2), 1401-1407.

Bean, J. C., & Hadj-Alouane, A. B. (1992). *A dual genetic algorithmfor bounded integer programs*. Tech. Rep., University of Michigan, Kalamazoo, Mich, USA.

Boonluk, P., Siritaratiwat, A., Fuangfoo, P., & Khunkitti, S. (2020). Optimal siting and sizing of battery energy storage systems for distribution network of distribution system operators. *Batteries*, *6*(4), 56.

Cazzola, P., Gorner, M., Schuitmaker, R., & Maroney, E. (2016). Global EV outlook 2016. *International Energy Agency, France*.

Coello, C. A. C. (2002). Theoretical and numerical constraint-handling techniques used with evolutionary algorithms: a survey of the state of the art. *Computer methods in applied mechanics and engineering*, *191*(11-12), 1245-1287.

Chinnam, R. B., & Murat, A. E. (2016). *Community-aware charging station network design for electrified vehicles in urban areas: Reducing congestion, emissions, improving accessibility, and promoting walking, bicycling, and use of public transportation* (No. TRCLC 15-08). Western Michigan University. Transportation Research Center for Livable Communities.

Deb, K. (2000). An efficient constraint handling method for genetic algorithms. *Computer methods in applied mechanics and engineering*, *186*(2-4), 311-338.

Deilami, S., Masoum, A. S., Moses, P. S., & Masoum, M. A. (2011). Real-time coordination of plug-in electric vehicle charging in smart grids to minimize power losses and improve voltage profile. *IEEE Transactions on smart grid*, *2*(3), 456-467.

Dixit, M., Kundu, P., & Jariwala, H. R. (2017). Incorporation of distributed generation and shunt capacitor in radial distribution system for techno-economic benefits. *Engineering Science and Technology, an International Journal*, *20*(2), 482-493.

Farsadi, M., Sattarpour, T., & Nejadi, A. Y. (2015, November). Optimal placement and operation of BESS in a distribution network considering the net present value of energy losses cost. In *2015 9th International Conference on Electrical and Electronics Engineering (ELECO)* (pp. 434-439). IEEE.

Fister, I., Fister Jr, I., Yang, X. S., & Brest, J. (2013). A comprehensive review of firefly algorithms. *Swarm and evolutionary computation*, *13*, 34-46.

Graham-Rowe, E., Gardner, B., Abraham, C., Skippon, S., Dittmar, H., Hutchins, R., & Stannard, J. (2012). Mainstream consumers driving plug-in battery-electric and plug-in hybrid electric cars: A qualitative analysis of responses and evaluations. *Transportation Research Part A: Policy and Practice*, *46*(1), 140-153.

Hung, D. Q., & Mithulananthan, N. (2012, July). Alternative analytical approaches for renewable DG allocation for energy loss minimization. In *2012 IEEE Power and energy society general meeting* (pp. 1-10). IEEE.

Islam, M. M., Mohamed, A., & Shareef, H. (2015, December). Optimal allocation of rapid charging stations for electric vehicles. In *2015 IEEE student conference on research and development (SCOReD)* (pp. 378-383). IEEE.

Islam, M. M., Shareef, H., & Mohamed, A. (2018). Optimal location and sizing of fast charging stations for electric vehicles by incorporating traffic and power networks. *IET Intelligent Transport Systems*, *12*(8), 947-957.

Joines, J. A., & Houck, C. R. (1994, June). On the use of non-stationary penalty functions to solve nonlinear constrained optimization problems with GA's. In *Proceedings of the first IEEE conference on evolutionary computation. IEEE world congress on computational intelligence* (pp. 579-584). IEEE.

Liu, X., Zhang, Q., & Cui, S. (2012). Review of electric vehicle V 2 G technology. *Diangong Jishu Xuebao(Transactions of China Electrotechnical Society)*, *27*(2), 121-127.

Michalewicz, Z., & Janikow, C. Z. (1991). Genetic algorithms for numerical optimization. *Statistics and Computing*, *1*, 75-91.

Matsuo, Y., Yanagisawa, A., & Yamashita, Y. (2013). A global energy outlook to 2035 with strategic considerations for Asia and Middle East energy supply and demand interdependencies. *Energy Strategy Reviews*, *2*(1), 79-91.

Cheung, N. J., Ding, X. M., & Shen, H. B. (2014). Adaptive firefly algorithm: parameter analysis and its application. *PloS one*, *9*(11), e112634.

Shaaban, M. F., Atwa, Y. M., & El-Saadany, E. F. (2012). PEVs modeling and impacts mitigation in distribution networks. *IEEE Transactions on Power Systems*, *28*(2), 1122-1131.

Tapia, R. (1986). Engineering Optimization: Methods and Applications (GV Reklaitis, A. Ravindran and KM Ragsdell). *SIAM Review*, *28*(2), 284. DOI:10.1137/1028097.

Singh, B. R., & Singh, O. (2012). *Global trends of fossil fuel reserves and climate change in the 21st century* (Vol. 8, pp. 167-192). chapter.

Teixeira, A. C. R., & Sodré, J. R. (2016). Simulation of the impacts on carbon dioxide emissions from replacement of a conventional Brazilian taxi fleet by electric vehicles. *Energy*, *115*, 1617-1622.

Yang, X. S., & He, X. (2013). Firefly algorithm: recent advances and applications. *International journal of swarm intelligence*, *1*(1), 36-50.

Yong, J. Y., Ramachandaramurthy, V. K., Tan, K. M., & Mithulananthan, N. (2015). Bi-directional electric vehicle fast charging station with novel reactive power compensation for voltage regulation. *International Journal of Electrical Power & Energy Systems*, *64*, 300-310.

Zitouni, F., Harous, S., & Maamri, R. (2021). A novel quantum firefly algorithm for global optimization. *Arabian journal for science and engineering*, *46*(9), 8741-8759.